JOURNAL OF BACTERIOLOGY, Feb. 1991, p. 1151–1160
0021-9193/91/031151-10$02.00/0

Vol. 173, No. 3

Identification of Three Amino Acid Residues in the B Subunit of Shiga Toxin and Shiga-Like Toxin Type II That Are Essential for Holotoxin Activity

L. P. PERERA, J. E. SAMUEL, R. K. HOLMES, AND A. D. O'BRIEN*

Department of Microbiology, Uniformed Services University of the Health Sciences, 4301 Jones Bridge Road, Bethesda, Maryland 20814-4799

Received 29 June 1990/Accepted 7 November 1990

Shiga toxin of *Shigella dysenteriae* type I and Shiga-like toxins I and II (SLT-I and SLT-II, respectively) of enterohemorrhagic *Escherichia coli* are functionally similar protein cytotoxins. These toxin molecules have a bipartite molecular structure which consists of an enzymatically active A subunit that inhibits protein synthesis in eukaryotic cells and an oligomeric B subunit that binds to globotriaosylceramide glycolipid receptors on eukaryotic cells. Regionally directed chemical mutagenesis of the B subunit of SLT-II was used to identify amino acids in the B subunit that are critical for SLT-II holotoxin cytotoxic activity. Three noncytotoxic mutants were isolated, and their mutations were mapped. The substitutions of arginine with cysteine at codon 32, alanine with threonine at codon 42, and glycine with aspartic acid at codon 59 in the 70-amino-acid mature SLT-II B polypeptide resulted in the complete abolition of cytotoxicity. The analogous arginine, alanine, and glycine residues were conserved at codons 33, 43, and 60 in the 69-amino-acid mature B polypeptide of Shiga toxin. Comparable mutations induced in the B-subunit gene of Shiga toxin by oligonucleotide-directed, site-specific mutagenesis resulted in drastically decreased cytotoxicity (10^3- to 10^6-fold) as compared with that of wild-type Shiga toxin. The mutant SLT-II and Shiga toxin B subunits were characterized for stability, receptor binding, immunoreactivity, and ability to be assembled into holotoxin.

Shiga toxin of *Shigella dysenteriae* type I and Shiga-like toxins (SLTs) of enterohemorrhagic *Escherichia coli* are protein cytotoxins with similar biological activities. Currently, two prototypes of SLTs have been described on the basis of antigenicity: Shiga-like toxin I (SLT-I) and Shiga-like toxin II (SLT-II) (31). SLT-I is almost identical to Shiga toxin at the nucleotide sequence level, whereas SLT-II shares approximately 55% overall nucleotide sequence homology with Shiga toxin (12). Porcine strains of *E. coli* implicated in edema disease of swine produce an SLT that is antigenically and genetically related to SLT-II of enterohemorrhagic *E. coli* but is classified as a variant of SLT-II (SLT-IIv) (20, 34) because it is cytotoxic for Vero but not HeLa cells. All of these cytotoxins are enterotoxic for ligated rabbit ileal segments and are lethal and paralytic for mice and rabbits.

Shiga toxin and the *E. coli* SLTs are bipartite toxins. The enzymatically active A subunit of each is associated with an oligomer of B subunits. The A subunit depurinates a specific adenine residue in the eukaryotic 28S rRNA in a manner identical to that of ricin and several other ribosome-inactivating proteins of plants (5). This depurination leads to inhibition of protein synthesis in eukaryotic cells (5). The oligomeric B subunits of Shiga toxin, SLT-I, and SLT-II bind to globotriaosylceramide (Gb_3) glycolipid receptors on eukaryotic cells, while the B subunit of SLT-IIv predominantly binds to the larger globotetraosylceramide (Gb_4) glycolipid receptor (17, 18, 24).

Although considerable progress has been made in the biochemical characterization of these toxins and the receptors to which they bind, the biophysical mechanisms involved in toxin-receptor interactions, subunit oligomerization, and holotoxin formation have not yet been defined. In this study, we used regionally directed, controlled chemical mutagenesis to identify three amino acids in the B subunit of SLT-II which are critical for holotoxin cytotoxicity. Because these three amino acids are conserved in the B subunits of Shiga toxin and SLT-IIv, mutations comparable to those induced by chemical mutagenesis of SLT-II were introduced in the Shiga toxin B subunit by oligonucleotide-directed, site-specific mutagenesis. Each of these mutations in Shiga toxin drastically reduced its cytotoxic activity, an observation which supports the hypothesis that each of these three amino acids plays a critical role in the holotoxin activities of Shiga toxin and the SLTs.

MATERIALS AND METHODS

Nomenclature. For the description of amino acids, the single-letter code was used. Mutations were designated as described by Knowles (15): the number defines the position of a mutation, and the substituted amino acid is given after the number.

Bacterial strains, media, and plasmid constructions. The *E. coli* strains and plasmids used in this study are listed in Table 1. All bacterial strains and transformants were grown in 2YT medium (19) with appropriate antibiotics. *E. coli* MV1190 was maintained on M9 glucose agar (19). All restriction enzymes were purchased from Boehringer Mannheim Biochemicals (Indianapolis, Ind.), unless otherwise indicated. Plasmid pNN76 (Table 1), which carries the SLT-II operon (*slt*-II), was described earlier by Newland et al. (22). This plasmid was cut with *Sph*I and *Kpn*I. The resultant 2.4-kb fragment with the entire *slt*-II operon was subcloned into the Bluescribe phagemid expression vector pBS(−) (Stratagene Cloning Systems, La Jolla, Calif.), and the resultant plasmid was designated pLP15. Plasmid pNAS13 carrying the Shiga

* Corresponding author.

TABLE 1. Bacterial strains and plasmids used in this study

Strain or plasmid	Description or genotype[a]	Reference or source
Strains		
CJ236	*dut-1 ung-1 thi-1 relA1*(pCJ105) (Cm^r)	16
DH5α	*supE44* Δ*lacU169* (ϕ80 *lacZ*ΔM15) *hsdR17 recA1 endA1 gyrA96 thi-1 relA1*	8
MV1190	*supE* Δ(*srl-recA*)*306*::Tn*10* (Tc^r) Δ(*lac-proAB*) *thi* (F′ *traD36 proAB lacI*^{q}ZΔM15)	16
Plasmids		
pBS(−)	Ap^r; phagemid expression vector	Stratagene
pNN76	pBR328 with *slt*-II; Ap^r	22
pLP15	pBS(−) with *slt*-II; Ap^r	This study
pNAS13	pBR329 with *stx*; Ap^r	29
pLPSH3	pNAS13 with *stx*; *Bgl*II-*Sal*I deletion upstream of *stx*; Ap^r	This study
pB5	pLPSH3 with *stx* deletion; Ap^r	This study

[a] Abbreviations: Tc^r, Cm^r, and Ap^r, resistance to tetracycline, chloramphenicol, and ampicillin, respectively.

toxin operon (*stx*) was described earlier by Strockbine et al. (29). This plasmid was cut with *Bgl*II and *Sal*I. The 5.9-kb fragment containing the entire *stx* operon was isolated by agarose gel electrophoresis. The termini of this fragment were blunted by treatment with single-strand-specific mung bean nuclease (Stratagene Cloning Systems). Following phenol-chloroform extraction and ethanol precipitation of DNA, the fragment was circularized by blunt-end ligation with T4 DNA ligase, and the resultant plasmid was designated pLPSH3 (Fig. 1). The 1.8-kb *Hin*dIII-*Eco*RI fragment of pLPSH3 was subcloned into the replicative-form M13mp18 vector to generate a single-stranded DNA template for oligonucleotide-directed, site-specific mutagenesis of the *stxB* gene.

Construction of gapped duplex DNA for mutagenesis. Plasmid pLP15 was transformed into *E. coli* DH5α by the Hanahan method (8). Purified plasmid DNA of pLP15 was made from the transformants by published procedures (19). Plasmid pLP15 DNA was cut with *Pst*I and *Eco*RI and subjected to gel electrophoresis, and a 5-kb fragment was isolated and purified by Geneclean (Bio 101 Inc., La Jolla, Calif.) in accordance with the instructions provided by the manufacturer. Plasmid pLP15 was also transformed into *E. coli* CJ236 by the Hanahan procedure (8). From these CJ236 transformants, purified pLP15 plasmid DNA with misincorporated uracil (pLP15 DNA-U) was made by standard procedures (19). The first step in constructing a gapped duplex with a single-strand region extending between the *Pst*I and *Eco*RI sites of pLP15 was to linearize pLP15 DNA-U with *Sph*I. Linearized pLP15 DNA-U (1.25 μg) was mixed with 0.5 μg of the gel-purified 5-kb fragment (*Pst*I-*Eco*RI) of pLP15 (obtained as described above) in 40 μl of 187.5 mM KCl–12.5 mM Tris (pH 7.5). To promote gapped duplex formation, we placed the mixture in boiling water for 3 min, incubated it at 65°C for 5 min, and allowed it to cool to room temperature for 45 min (Fig. 2).

Sodium bisulfite mutagenesis of gapped duplex DNA. Fifty microliters (approximately 20 μg/ml) of gapped duplex DNA of pLP15 in 15 mM NaCl–1.5 mM sodium citrate (pH 7.0) was mixed with 150 μl of freshly prepared 4 M sodium bisulfite solution (pH 6.0) and 2 μl of freshly prepared 50 mM hydroquinone. One hundred microliters of paraffin oil was layered above the mixture, which was then incubated at 37°C for 1 h in the dark. The mutagenesis reaction was stopped by removing the sodium bisulfite through dialysis as described by Shortle and Botstein (28). The dialyzed sample was extracted three times with ether to remove paraffin oil, and 50 μg of tRNA (Sigma Chemical Co., St. Louis, Mo.) was added to facilitate precipitation of the DNA with ethanol. The DNA pellet was resuspended in 10 μl of 20 mM Tris hydrochloride (pH 7.4)–2 mM $MgCl_2$–50 mM NaCl. The resuspended DNA was placed on ice for 5 min before the addition of 1 μl of 10× synthesis buffer (Bio-Rad Laboratories, Richmond, Calif.; containing 5 mM each dATP, dCTP, dGTP, and dTTP, 10 mM ATP, 100 mM Tris [pH 7.4], 50 mM $MgCl_2$, and 20 mM dithiothreitol), 5 U of T4 DNA ligase, and 1 U of T4 DNA polymerase (Bio-Rad Laboratories). The sample was incubated for 5 min on ice, for 5 min at 25°C, and for 90 min at 37°C to fill in the single-strand gap in vitro. *E. coli* MV1190 was transformed with 10 μl of the regionally mutagenized pLP15 DNA.

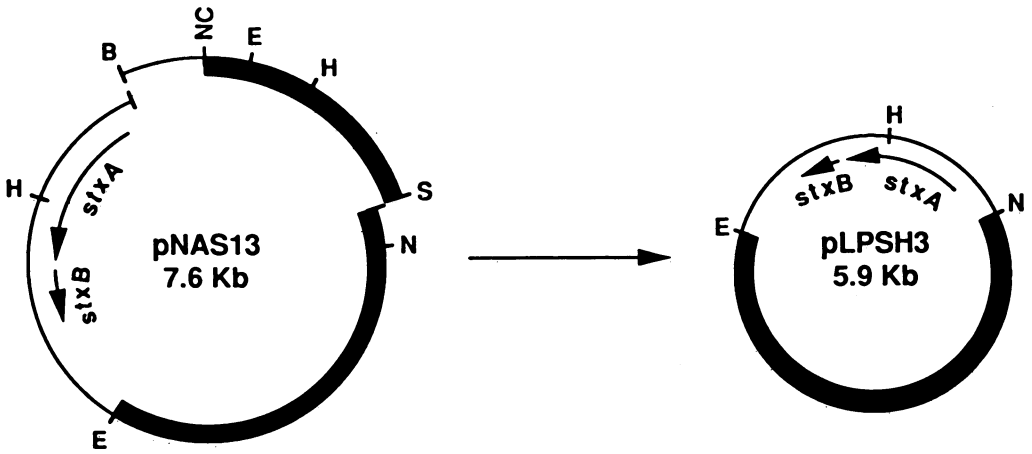

FIG. 1. Construction of pLPSH3. The 7.6-kb plasmid pNAS13, which carries the *stx* operon, was digested with *Bgl*II and *Sal*I. The 5.9-kb fragment containing the entire *stx* operon was isolated, treated with mung bean nuclease to blunt the termini, and circularized by blunt-end ligation to form pLPSH3. Abbreviations for the restriction endonuclease sites: E, *Eco*RI; H, *Hin*dIII; B, *Bgl*II; S, *Sal*I; N, *Nru*I; NC, *Nco*I.

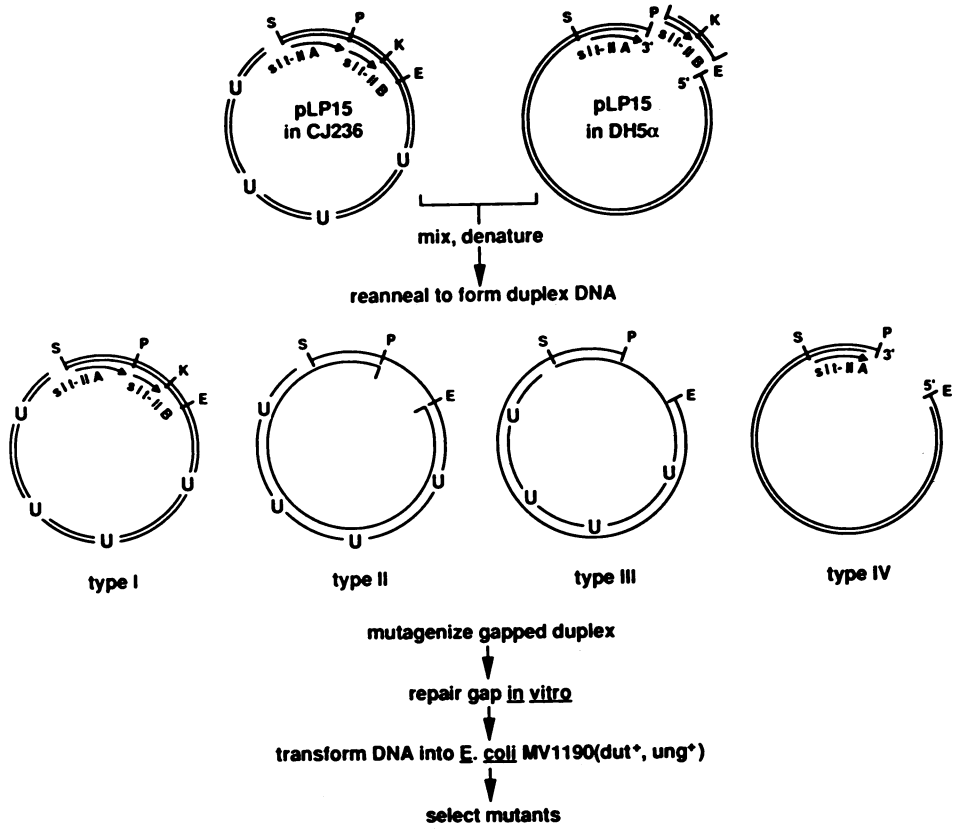

FIG. 2. Schematic outline of the method for generating gapped duplex DNA molecules for single-strand-specific sodium bisulfite mutagenesis and enrichment for mutant selection. *Sph*I-linearized pLP15 DNA-U was mixed with pLP15 from which the *slt*-IIB gene had been excised. Following denaturation and renaturation of the mixture, the gapped duplex DNA was subjected to mutagenesis. The gaps were repaired in vitro, and the DNA was used to transform *E. coli* MV1190 (*dut*$^+$ *ung*$^+$). Mutants with reduced cytotoxicity were selected. This protocol favors the progeny of type II and III molecules because type I molecules contain misincorporated uracil in both strands and are rapidly degraded in *E. coli* MV1190 and type IV molecules do not form covalently closed circular molecules for efficient transformation. Abbreviations for the restriction endonuclease sites: S, *Sph*I; P, *Pst*I; K, *Kpn*I; E, *Eco*RI.

Cytotoxicity assays on Vero and HeLa cells. Cytotoxicity assays were performed essentially as described previously (6), with the exception that the tissue culture medium contained 50 μg of gentamicin per ml. In brief, transformants were grown overnight at 37°C with vigorous shaking in 1 ml of 2YT with 200 μg of ampicillin per ml. After pelleting of the bacteria by centrifugation (10,000 × *g* for 5 min), the culture supernatant was added to freshly seeded HeLa or Vero cells in 96-well microtiter plates (1 μl of bacterial culture supernatant per well in duplicate). The cytotoxicities of the mutants were titrated by 10-fold serial dilutions. The highest toxin dilution that caused lysis of 50% of the cell monolayer (CD_{50}) was taken as the titer of each toxin.

DNA sequencing. CsCl density gradient-purified plasmid DNA was sequenced with the Sequenase DNA sequencing kit (US Biochemical Corp., Cleveland, Ohio) in accordance with the double-stranded DNA sequencing protocol provided by the manufacturer but with the modification that 1 μl of undiluted Sequenase enzyme was used in each sequencing reaction.

Oligonucleotide-directed, site-specific in vitro mutagenesis. Oligonucleotide-directed, site-specific mutagenesis was done with the Muta-Gene in vitro mutagenesis kit (Bio-Rad Laboratories) in accordance with the manufacturer's instructions. M13mp18 with the 1.8-kb *Hin*dIII-*Eco*RI DNA fragment of the *stx* operon was used to generate single-stranded DNA templates for in vitro mutagenesis. This recombinant phage yields the noncoding strand of the *stxB* gene, and the following synthetic mutagenic oligonucleotides that correspond to the coding strand of *stxB* (substituted bases are underlined) were used to generate mutations at codons 33, 43, and 60 of the mature B subunit of Shiga toxin: 5′ TTATTTACCAACTGCTGGAATCTTCAG 3′ (AGA changed to TGC at position 33); 5′ CTTCTTCTCAGTACG CAAATTACGGGG 3′ (GCG changed to ACG at position 43); and 5′ GCCTGTCATAATGACGGGGGATTCAGC 3′ (GGA changed to GAC at position 60). Introduction of mutations was confirmed by DNA sequencing. Replicative-form DNAs of M13mp18 recombinants that carried the mutations were digested with *Hin*dIII and *Eco*RI. To reconstruct the mutant *stx* operon, we isolated the 1.8-kb *Hin*dIII-*Eco*RI fragments and ligated them to the 4.1-kb *Hin*dIII-*Eco*RI fragment of pLPSH3, which contained the rest of the *stx* operon (Fig. 1).

Pulse-chase analysis of toxin mutants. Pulse-chase experiments (2) were done to compare the rate of degradation of SLT-II, Shiga toxin, and toxin mutants within the bacterial host. *E. coli* transformed with plasmid pLP15 (SLT-II) or pLPSH3 (Shiga toxin) and *E. coli* that carried plasmids with mutated toxin genes were grown overnight at 37°C in M9 medium with 1% Casamino Acids, 0.1 μg of thiamine per ml (25), and 200 μg of ampicillin per ml. Bacterial cells were

washed twice with Hershey salt solution (26) and resuspended in sulfate-free Hershey medium with 200 μg of ampicillin per ml. The cultures were diluted 50-fold in 3 ml of Hershey medium and allowed to grow at 37°C with agitation until the optical density at 600 nm was approximately 0.5. The bacterial cultures were pulsed with 3 μl of [^{35}S]methionine (>800 Ci/mmol; 15 μCi/μl) for 5 min, and excess unlabeled methionine (0.01 M) was added. Aliquots (500 μl) of the bacterial cultures were removed at predetermined intervals and mixed immediately with 35 μl of ice-cold protease inhibitor solution (60 mM phenylmethyl sulfonyl fluoride, 30 mM *N*-ethylmaleimide, 80 mM NaN_3) on ice. The bacterial cells were pelleted by centrifugation (10,000 × *g* for 2 min) and resuspended in 50 μl of lysis buffer (100 mM Tris hydrochloride [pH 8], 1 mM EDTA, 10 mM 2-mercaptoethanol, 500 mM NaCl, 6 M urea, 0.1% Nonidet P-40, 0.0125% bromophenol blue). The lysed bacterial cells were boiled for 5 min and subjected to sodium dodecyl sulfate-polyacrylamide gel electrophoresis with 15% polyacrylamide. The gel was treated with Enlightning (NEN Research Products, Boston, Mass.), dried, and subjected to autoradiography to visualize labeled proteins. Densitometric scans of the autoradiograms were done on a model 230M Datacopy Scanner with the MacImage program (Xerox Imaging Systems Inc., Mountain View, Calif.).

Dot blot ELISA. The immunoreactivities of the mutant SLT-II and Shiga toxin polypeptides with monoclonal antibodies (MAb) against the B subunits of SLT-II and Shiga toxin were determined by a previously described (33) dot blot enzyme-linked immunosorbent assay (ELISA), with several modifications as outlined below. *E. coli* producing wild-type or mutant toxin was grown overnight at 37°C in 50 ml of 2YT containing 200 μg of ampicillin per ml. The bacterial cultures were placed on ice and subjected to sonic lysis (Ultratip Labsonic System; Lab-Line Instruments, Mentrose Park, Ill.). To limit proteolysis, we added 0.3 mM phenylmethylsulfonyl fluoride to the sonically disrupted cultures. The cellular debris was removed by centrifugation at 10,000 × *g* for 15 min at 4°C. The supernatants of the sonic lysates were further concentrated by 60% ammonium sulfate precipitation of proteins. The precipitates were resuspended in 0.5 ml of phosphate-buffered saline (PBS). The residual ammonium sulfate was removed by overnight dialysis in 3 liters of PBS, and the total protein content of the sonic lysates was standardized. A dot blot apparatus (Schleicher & Schuell Inc., Keene, N.H.) connected to a vacuum was used to spot 10 μl of concentrated sonic lysate on a nitrocellulose membrane. The nitrocellulose membrane was air dried and immersed for 1 h at room temperature in Tris-buffered saline (200 mM Tris hydrochloride [pH 7.5], 150 mM NaCl) with 1% bovine serum albumin to saturate the membrane and prevent proteins from nonspecifically binding to the membrane during subsequent incubations. The membrane was transferred to 20 ml of a 1:5 dilution of MAb culture supernatant or a 1:2,500 dilution of MAb ascitic fluid and incubated for 1 h at room temperature. All antibody dilutions were made in Tris-buffered saline with 1% bovine serum albumin. The membrane was washed five times in 20 ml of Tris-buffered saline with 0.05% Tween 20 and incubated for 1 h at room temperature in 20 ml of a 1:3,000 dilution of alkaline phosphatase-conjugated goat antimouse immunoglobulin G (IgG)-IgM IgA antibody (Bethesda Research Laboratories, Gaithersburg, Md.). The unbound second antibody was removed by five washes with Tris-buffered saline with 0.05% Tween 20 as described above. The membrane was immersed in 10 ml of chromogen solution containing 0.3 mg of Nitro Blue Tetrazolium per ml and 0.15 mg of 5-bromo-4-chloro-3-indolyl phosphate (BCIP) per ml in 100 mM Tris hydrochloride [pH 9.5]–100 mM NaCl–5 mM $MgCl_2$. The color development was allowed to proceed in the dark for 15 min, after which the membrane was washed once in 20 ml of 20 mM Tris hydrochloride [pH 2.9] containing 1 mM EDTA. The specificities of the MAb used in the dot blot ELISA were as follows: BC5 reacts with the B subunit of SLT-II (4), and 13C4, 19G8, and 16E6 react with the B subunit of Shiga toxin (30).

Receptor analog ELISA. The toxin mutants were tested for their ability to bind to the receptor analog by a previously described (34) ELISA. The receptor analog, obtained from Carbohydrates International, Chicago, Ill., was (Galα1-4Galβ-O-CETE)$_n$bovine serum albumin (BSA) (30 to 40 mol of disaccharide per mol of BSA), where CETE is 2-(2-carbomethoxyethylthio)ethyl linker. In brief, 1:5, 1:50, and 1:100 dilutions of wild-type or mutants toxin were incubated at 4°C overnight with the receptor analog anchored to a solid phase. The unbound toxin was removed by washing, and the receptor-bound toxin was detected with a toxin-specific MAb.

TLC overlay assay. The thin-layer chromatogram (TLC) overlay assay was done essentially as described earlier (24). In brief, total glycolipid extracts from HeLa and Vero cells as well as purified neutral and acidic glycolipids, which served as controls, were chromatographed on aluminum-backed silica gel high-performance TLC plates (Silica Gel 60; E. Merck AG, Darmstadt, Federal Republic of Germany). The chromatograms were air dried before being soaked in TBS-BSA buffer (100 mM Tris hydrochloride [pH 7.8] containing 150 mM NaCl and 1% bovine serum albumin) for 2 h at room temperature. The plates were overlaid with the toxins in TBS-BSA buffer and incubated for 18 h at 4°C. After five washes in cold PBS, the plates were overlaid with a toxin-specific MAb for 1 h at room temperature. The unbound MAb was removed by washing the plates with PBS before adding ^{125}I-labeled goat antimouse IgG in TBS-BSA buffer. The plates were incubated at room temperature for 1 h, washed four times in cold PBS, air dried, and subjected to autoradiography.

Immunofluorescence assay. An immunofluorescence assay was developed to detect the binding of mutant toxins to Vero cells. Freshly dispersed Vero cells were suspended to a concentration of 10^5 cells per ml of diluent buffer (Earle balanced salt solution with 10% fetal calf serum and 0.1% NaN_3). Fifty microliters of the concentrated bacterial cell lysate with wild-type or mutant toxin (prepared as described above for the dot blot ELISA) was added to 450 μl of the Vero cell suspension. The cell suspension was incubated at 4°C for 1 h with gentle agitation. The cells were washed three times by centrifugation (1,000 × *g* for 3 min at 4°C) in 1 ml of washing buffer (Earle balanced salt solution with 1% fetal calf serum and 0.1% NaN_3) and resuspended in 495 μl of diluent buffer. Five microliters of toxin-specific MAb (ascitic fluid) was added. The MAb was incubated with the cell suspension for 45 min at 4°C with gentle agitation. Excess unbound MAb was removed by washing as described above. Next, the cells were resuspended in 495 μl of diluent buffer, and 5 μl of fluorescein-conjugated goat antimouse F(ab')$_2$ was added (Cappel Laboratories, Westchester, Pa.). The cells were incubated at 4°C for 45 min, washed three times with washing buffer, and washed once with Earle balanced salt solution with 0.1% NaN_3 but without fetal calf serum. The cells were differentially labeled with the cell membrane-intercalating fluorescence dye dil (1-1'dioctadecyl-3-3,3'3'-

tetramethyl iodocarbocyanine perchlorate) (Molecular Probes, Eugene, Oreg.) as described by Hogan et al. (10) for nonspecific fluorescence imaging of cells. The cells were transferred to a flat-bottom 96-well microtiter plate (100 μl of cell suspension per well), and the plate was subjected to centrifugation at 1,000 × *g* for 3 min to disperse the cells into a monolayer. During the entire assay, cells were maintained at 4°C with NaN_3 to prevent internalization of cell-bound ligands. Fluorescence analysis of cell-bound toxins was accomplished with Anchored Cell Analysis Station 470 (ACAS 470; Meridian Instruments Inc., Okemos, Mich.) essentially as described by Hogan et al. (10) for a different system.

Inoculation of mice and rabbits. To determine whether the noncytotoxic SLT-II mutants were also lethal for mice, we inoculated concentrated sonic lysates of *E. coli* that expressed mutant SLT-II (prepared as described above for the dot blot ELISA) intraperitoneally into BALB/c mice. Each crude mutant toxin preparation was inoculated into a group of five mice (100 μl of sonic lysate per mouse). As a positive control for toxicity, a group of five mice was inoculated with a concentrated sonic lysate of *E. coli*(pLP15) that expressed wild-type SLT-II (100 μl of sonic lysate per mouse). To assess the feasibility of using the noncytotoxic SLT-II mutants to raise neutralizing antibodies against SLT-II, we inoculated three rabbits intramuscularly (500 μl of concentrated sonic lysate per rabbit) with the SLT-II mutant toxin preparations (one rabbit per mutant). The first inoculum was administered with complete Freund's adjuvant, and three subsequent inocula were administered at monthly intervals with incomplete Freund's adjuvant. The three rabbits were bled, and the sera from them were tested for neutralizing antibodies against SLT-II by the cytotoxicity neutralization assay.

RESULTS

Sodium bisulfite mutagenesis of gapped duplex DNA. The strategy for generation of gapped duplex DNA molecules from pLP15, mutagenesis of gapped duplex DNA, and selection for mutations in the *slt*-IIB gene is outlined in Fig. 2. When *Sph*I-linearized pLP15 DNA-U was mixed with pLP15 plasmid DNA from which the target *slt*-IIB region had been excised, four types of duplex molecules were, in principle, formed after renaturation (Fig. 2; types I to IV). This mixture of duplex molecules was subjected to sodium bisulfite mutagenesis. The rate of mutagenesis of the *slt*-IIB target region was controlled by varying the concentration of sodium bisulfite used in the reaction. A concentration of 3 M sodium bisulfite was found to be optimal. The type II and III molecules represented sense and antisense strands of the target region simultaneously subjected to mutagenesis. When the four types of mutagenized gapped duplex DNA were subjected to gap repair and the DNA was transformed into *E. coli* MV1190 (*dut*$^+$ *ung*$^+$), strong selection was exerted against type I molecules with misincorporated uracil in both strands. The inability to form covalently closed circular molecules greatly diminished the transformation efficiency of type IV molecules. The transformants were screened for cytotoxicity. From a total of 800 transformants screened, 3 mutants which completely lacked any detectable cytotoxicity on both Vero and HeLa cells were isolated. The loss of any detectable cytotoxicity in these mutants represented at least a 10,000-fold reduction in cytotoxicity when compared with the cytotoxicity of the parental strain (Table 2). Furthermore, the sonic lysates of these *E. coli* strains expressing the mutant toxins were not cytotoxic even after concentration of the lysates 100-fold with ammonium sulfate (data not shown).

TABLE 2. Vero cell cytotoxicity and immunoreactivity of the SLT-II and Shiga toxin mutants

Toxin	Vero cell cytotoxicity (CD_{50})	Immunoreactivity with MAb[a]:			
		13C4	16E6	19G8	BC5
SLT-II[b]	10^4–10^5	NA	NA	NA	+++
SLT-II R32C	<10	NA	NA	NA	−
SLT-II A42T	<10	NA	NA	NA	++
SLT-II G59D	<10	NA	NA	NA	++
Shiga toxin[c]	10^9–10^{10}	+++	+++	+++	NA
Shiga R33C	10^1–10^2	+++	+++	+++	NA
Shiga A43T	10^4–10^5	±	±	±	NA
Shiga G60D	10^3–10^4	+++	+++	−	NA

[a] MAb 13C4, 16E6, and 19G8 are specific for the B subunit of Shiga toxin (30). MAb BC5 is specific for the B subunit of SLT-II (4). Immunoreactivity (determined by the dot blot ELISA; see Material and Methods for details) with MAb is indicated as follows: NA, not applicable; +++, strong reaction; ++, moderate reaction; ±, weak reaction; −, negative reaction.

[b] Tenfold serial dilutions of the lysate containing wild-type SLT-II were tested in the dot blot ELISA with MAb BC5 as a probe. Immunoreactivity was lost at a 1:1,000 dilution of the toxin.

[c] Tenfold serial dilutions of the lysate containing wild-type Shiga toxin were tested in the dot blot ELISA with MAb 13C4 as a probe. Immunoreactivity was lost at a 1:1,000 dilution of the toxin.

Sequence analysis and oligonucleotide-directed, site-specific mutagenesis. Sequence analysis of the noncytotoxic SLT-II mutants revealed that each of the three mutants contained a single point missense mutation in the *slt*-IIB gene targeted in the regionally directed mutagenesis. In the mature B subunit of SLT-II, the three independent mutations mapped to codons 32, 42, and 59 of the 70-amino-acid polypeptide. Codon 32, CGC, which codes for arginine (R), was mutated to TGC, which codes for cysteine (C) (mutant SLT-II R32C). Codon 42, GCT, which codes for alanine (A), was mutated to ACT, which codes for threonine (T) (mutant SLT-II A42T). Codon 59, GGC, which codes for glycine (G), was mutated to GAC, which codes for aspartic acid (D) (mutant SLT-II G59D). In the R32C mutation, cytosine in the sense strand had undergone deamination by bisulfite, whereas in the A42T and G59D mutations, cytosine in the antisense strand had undergone deamination by bisulfite. The abrogation of cytotoxicity in these mutants suggests an important role for the arginine, alanine, and glycine residues at these respective positions in mediating the cytotoxic activity of the SLT-II holotoxin. Furthermore, these three amino acids are conserved in the 69-amino-acid polypeptide of the B subunit of Shiga toxin. Because of an additional proline in the N terminus of Shiga toxin, the analogous codons in Shiga toxin are codons 33, 43, and 60 (29).

To determine whether these three residues are critical for the cytotoxic activity of Shiga toxin, we induced identical mutations by oligonucleotide-directed, site-specific mutagenesis in M13mp18 recombinants carrying *stxB*. The reconstruction of each mutant *stx* operon (wild-type A-subunit gene with mutated B-subunit gene) was facilitated by the construct pLPSH3 (Fig. 1), in which the *Hin*dIII and *Eco*RI sites on the vector upstream of the *stx* gene in pNAS13 were eliminated. All three mutations caused a 10^4-fold or greater reduction in cytotoxic activity when compared with the cytotoxicity of the wild-type Shiga toxin (Table 2). Thus, in contrast to the corresponding SLT-II mutants, Shiga R33C, Shiga A43T, and Shiga G60D still retained detectable cyto-

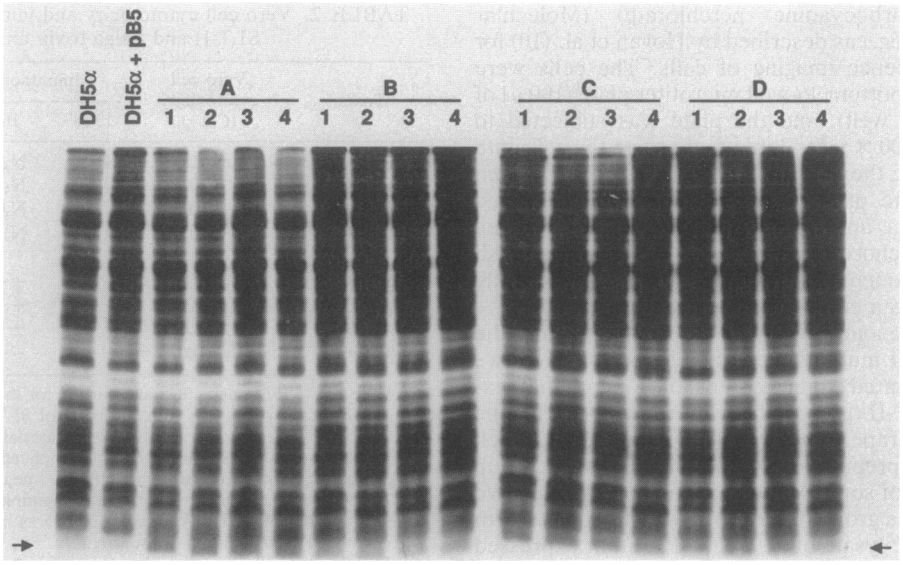

FIG. 3. Pulse-chase analysis of intracellular degradation of Shiga toxin mutants. *E. coli* expressing wild-type Shiga toxin or Shiga toxin mutants was pulse-labeled with [^{35}S]methionine for 5 min as described in Materials and Methods. The labeled bacterial cells were harvested at 5 min (lanes 1), 15 min (lanes 2), 30 min (lanes 3), and 60 min (lanes 4) after the cold methionine chase. The cells were lysed by being boiled and were subjected to sodium dodecyl sulfate-polyacrylamide gel electrophoresis as described in Materials and Methods. The arrow indicates the position of the Shiga toxin B polypeptide. (A) Lysates containing wild-type Shiga toxin. The relative mean intensities of the band at the arrow as assessed by scanning were as follows: lane 1, 27; lane 2, 27; lane 3, 29; and lane 4, 27. (B) Lysates of mutant Shiga R33C. The relative mean intensities of the band at the arrow as assessed by scanning were as follows: lane 1, 24; lane 2, 29; lane 3, 26; and lane 4, 27. (C) Lysates of mutant Shiga A43T. The relative mean intensities of the band at the arrow as assessed by scanning were as follows: lane 1, 52; lane 2, 55; lane 3, 46; and lane 4, 49. (D) Lysates of mutant Shiga G60D. The relative mean intensities of the band at the arrow as assessed by scanning were as follows: lane 1, 44; lane 2, 55; lane 3, 48; and lane 4, 45. Lysates of *E. coli* DH5α labeled for 5 min and *E. coli* DH5α(pB5) (pLPSH3 without the *stx* operon) labeled for 5 min were included as controls.

toxic activity. However, the fold reduction in the cytotoxic activities of both SLT-II and Shiga toxin mutants was similar when compared with the cytoxicity of the respective wild-type toxin (Table 2).

Intracellular degradation of Shiga toxin mutants. Pulse-chase experiments were done to eliminate the possibility that the ablated or reduced activities of the toxin mutants were due to enhanced susceptibility to intracellular proteolytic degradation. The B subunit of Shiga toxin was identified by its molecular weight (Fig. 3, arrow) and by the absence of a band corresponding to this polypeptide in lanes that contained labeled lysates of *E. coli* DH5α or *E. coli* DH5α(pB5). Shiga toxin and the three mutants had apparent intracellular half-lives longer than 60 min, as determined visually and confirmed by densitometric scanning (Fig. 3) of the position on the autoradiogram that corresponded to the B subunit. This finding favors the hypothesis that the reduced cytotoxicity of these mutants is due to attenuation of activity rather than to instability of the toxin. The stability of SLT-II mutants could not be determined because the larger B subunit of SLT-II comigrated with host cell proteins in the pulse-chase experiment (data not shown).

Dot blot ELISA. The immunoreactivity of the mutant Shiga toxins with B-subunit-specific-MAb was analyzed with a dot blot ELISA (Table 2). MAb 13C4, 16E6, and 19G8 recognize conformation-dependent epitopes on the B subunit of Shiga toxin (31). All three MAb reacted strongly with mutant Shiga R33C. Mutant Shiga A43T reacted weakly with MAb 13C4 but did not react with the other two MAb. Mutant Shiga G60D reacted with both MAb 13C4 and 16E6 but failed to react with MAb 19G8, indicating that the G60D mutation inactivated the epitope reactive with MAb 19G8. The SLT-II mutants were probed with MAb BC5 specific for the B subunit of SLT-II. Mutant SLT-II R32C did not react with MAb BC5, while mutants SLT-II A42T and SLT-II G59D did react with that MAb, but not to the same extent as did wild-type SLT-II (Table 2). This finding indicates that the epitope reactive with MAb BC5 was not drastically altered by the A42T or the G59D mutation.

Receptor analog ELISA. To assess whether the mutations in the B subunit of Shiga toxin affected the receptor-binding ability of the B subunit, we tested the Shiga toxin mutants in a receptor analog ELISA. MAb 13C4 was used as a probe to detect receptor analog-bound toxin. Even at the highest concentration of mutant toxin tested, mutant Shiga R33C failed to bind to the receptor analog, suggesting that the R33C mutation had abrogated the receptor-binding capacity of the B subunit of Shiga toxin (Fig. 4). Mutant Shiga A43T bound to the receptor analog very weakly (Fig. 4). To exclude the possibility that this apparent weak binding was really due to less avid antigen-antibody interactions (see immunoreactivity results in Table 1), we repeated the assay with MAb 4F7 specific for the A subunit of Shiga toxin (7) as a probe for receptor analog-bound holotoxin. A marked reduction in the binding of mutant Shiga A43T to the receptor analog was still observed (data not shown). By contrast, the binding of mutant Shiga G60D to the receptor analog was almost comparable to that of the wild-type Shiga toxin at high concentrations but, as the toxin was diluted, mutant Shiga G60D displayed a more precipitous reduction in receptor-binding ability than did the wild-type Shiga toxin (Fig. 4). When SLT-II mutants were tested in the receptor analog ELISA, none of the three mutants elicited any signal above the background when a B-subunit-specific MAb (BC5)

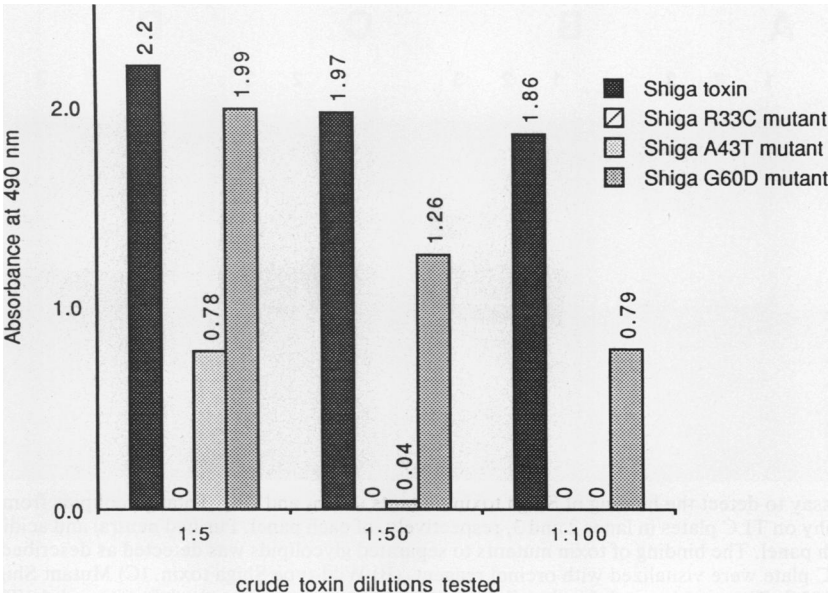

FIG. 4. Binding of Shiga toxin mutants to the receptor analog. Different dilutions of concentrated sonic lysates of *E. coli* that expressed Shiga toxin and Shiga toxin mutants were tested for receptor analog binding by a receptor analog ELISA as described in Materials and Methods. The receptor analog-bound toxin was detected with MAb 13C4, which is specific for the B subunit of Shiga toxin (30). Mutant Shiga R33C did not elicit any signal, even at the highest concentration tested. The absorbance values given in the graph are the averages of three separate experiments.

or an A-subunit-specific MAb (11E10) (23) was used as a probe to detect receptor analog-bound toxin (Table 3).

TLC overlay assay. The Shiga toxin mutants were tested in a TLC overlay assay to examine any differences in binding to the entire glycolipid moiety rather than to a receptor analog. Mutant Shiga R33C did not bind to Gb_3, Gb_4, or any other glycolipid in total glycolipid extracts of Vero or HeLa cells. The binding profile of mutant Shiga A43T revealed a drastic reduction in binding to Gb_3 and Gb_4, but no aberrant glycolipid binding was evident. The binding profile of mutant Shiga G60D resembled that of the wild-type Shiga toxin (Fig. 5). The three SLT-II mutants did not elicit any significant binding to Gb_3 in the TLC overlay assay (Table 3).

Immunofluorescence assay. Shiga toxin mutants were tested in an indirect immunofluorescence assay. Both binding of B subunits to Vero cells and the assembly of A and B subunits into holotoxin were required to elicit fluorescence, since MAb 4F7 used for the detection of bound toxin was specific for the A subunit of Shiga toxin and since this subunit is incapable of binding to Vero cells directly (3). During the entire assay, cells were maintained in buffer with sodium azide at 4°C to prevent any internalization of bound toxin. The fluorescence of differentially labeled cells in the scanned field by the cell membrane-intercalating fluorescence dye dil is depicted in the detector 2 row of Fig. 6. The toxin-specific fluorescence elicited by the wild-type Shiga toxin (pLPSH3) is shown in Fig. 6E. Mutant Shiga R33C did not show significant toxin-specific fluorescence (Fig. 6B), whereas mutant Shiga G60D showed significant toxin-specific fluorescence (Fig. 6D). By contrast, mutant Shiga A43T showed strong toxin-specific fluorescence which was almost comparable in intensity to that shown by the wild-type Shiga toxin (compare Fig. 6C and E). No toxin-specific fluorescence was detected for any of the three SLT-II mutants when an MAb specific for the A subunit (11E10) or the B subunit (BC5) was used as a probe to detect toxin bound to Vero cells (Table 3).

TABLE 3. Binding of SLT-II mutants to the receptor analog, Gb_3, and Vero cells

Toxin	Binding of SLT-II mutants to[a]:		
	Receptor analog[b]	Gb_3[c]	Vero cells[d]
SLT-II	+++	+++	+++
SLT-II R32C	−	±	±
SLT-II A42T	−	−	−
SLT-II G59D	−	±	±

[a] +, Strong binding; ±, marginal binding; −, no detectable binding.
[b] Determined by the receptor analog ELISA.
[c] Determined by the TLC overlay assay.
[d] Determined by the immunofluorescence assay with ACAS 470.

Animal inoculations with SLT-II mutants. To determine whether the ablation of the Vero cell cytotoxicity of the SLT-II mutants correlated with a decreased toxicity for animals, we inoculated BALB/c mice and rabbits with concentrated sonic lysates of *E. coli* expressing SLT-II mutants. Mice inoculated with lysates that contained SLT-II mutants survived, whereas mice inoculated with sonic lysates of *E. coli*(pLP15) died 4 to 5 days postinoculation. Rabbits inoculated with SLT-II mutants also survived, and after three inoculations, the sera from the rabbits inoculated with all three SLT-II mutants contained neutralizing antibodies against SLT-II (data not shown). The Shiga toxin mutants were not evaluated for lethality for mice or rabbits, since all three mutants retained cytoxicity levels over and above the reported lethal dose for these animals.

DISCUSSION

The toxin-receptor interactions of Shiga toxin and the SLTs have been investigated by several groups of investiga-

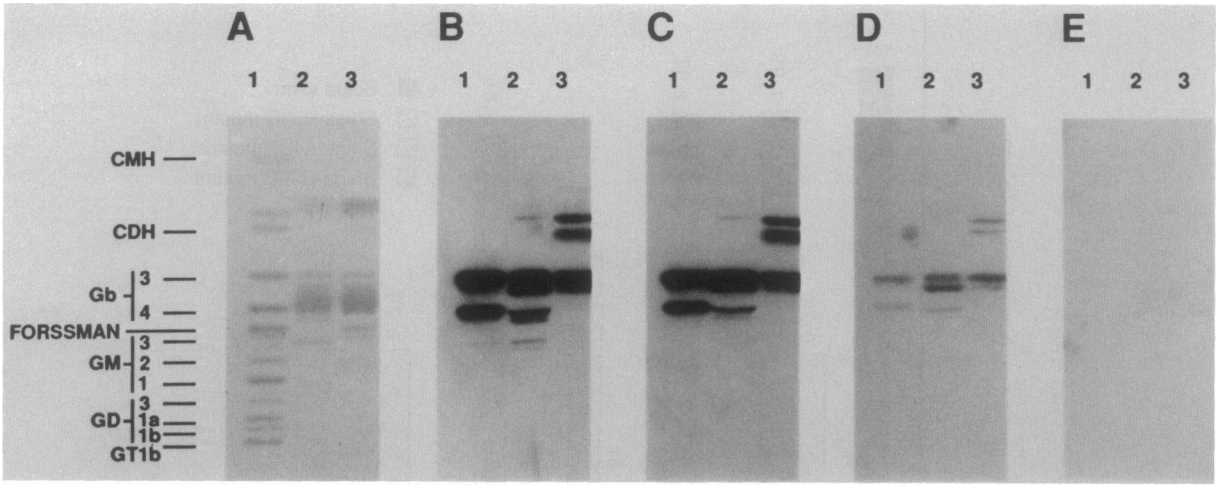

FIG. 5. TLC overlay assay to detect the binding of Shiga toxin mutants to Gb_3 and Gb_4. Total glycolipids from Vero and HeLa cells were subjected to chromatography on TLC plates in lanes 2 and 3, respectively, of each panel. Purified neutral and acidic glycolipids were included as controls in lane 1 of each panel. The binding of toxin mutants to separated glycolipids was detected as described in Materials and Methods. (A) Glycolipids on the TLC plate were visualized with orcinol reagent. (B) Wild-type Shiga toxin. (C) Mutant Shiga G60D. (D) Mutant Shiga A43T. (E) Mutant Shiga R33C. The positions of the glycolipid standards are indicated to the left of panel A. The standards are defined in reference 24.

tors (2a, 11, 17, 18, 21, 32a). Recently, Jackson et al. (13) from this laboratory used oligonucleotide-directed, site-specific mutagenesis to change one or two amino acids at a time in the B polypeptides of Shiga toxin and SLT-IIv in an attempt to identify the amino acids involved in binding to Gb_3 and Gb_4, respectively. Although none of the single-amino-acid substitutions significantly reduced the cytotoxicity of either toxin, double mutations and the introduction of terminator codons identified three domains of the Shiga toxin B subunit that appear to be critical for toxin-receptor interactions and/or holotoxin assembly. These regions include the hydrophilic area near the amino terminus, the last five amino acids at the carboxy terminus, and the single disulfide bond. Harari et al. (9) also implicated that the conserved hydrophilic region of the Shiga toxin B subunit is important for binding by generating cytotoxin-neutralizing antibodies with synthetic peptides corresponding to that region. However, these investigators did not show that the neutralizing antibodies interfered with toxin-receptor interactions. In the present study, we used regionally directed chemical mutagenesis to identify amino acids in the B subunit of SLT-II important for the cytotoxic activity of the holotoxin. The mutants were characterized to determine if the loss of cytotoxic activity was the result of a change either in the receptor-ligand interaction or in holotoxin assembly.

Regionally directed sodium bisulfite mutagenesis has been

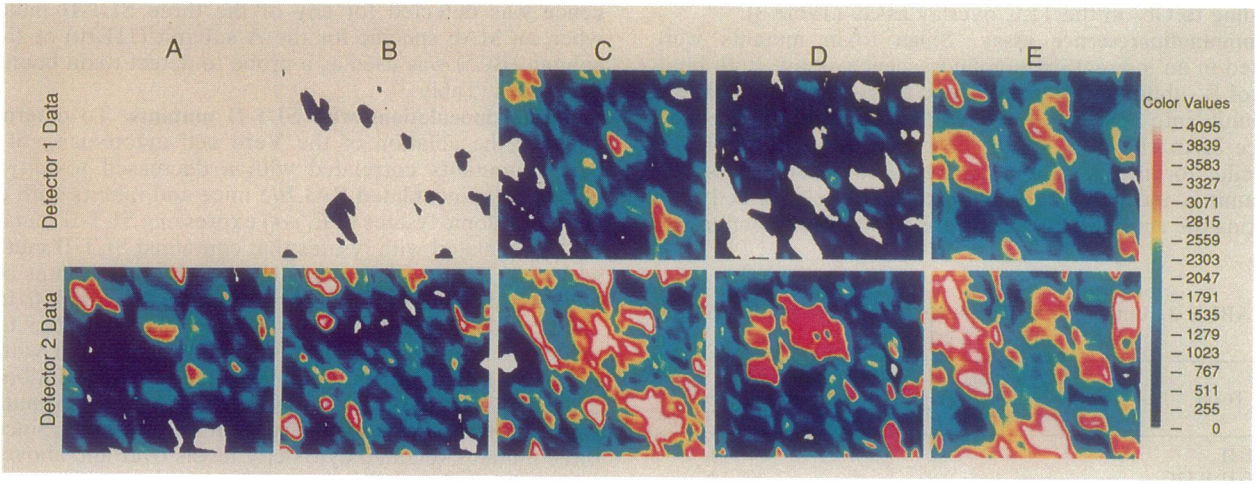

FIG. 6. Binding of Shiga toxin mutants to Vero cells as detected by the immunofluorescence assay with the ACAS 470. Concentrated sonic lysates of *E. coli* that expressed Shiga toxin or Shiga toxin mutants were incubated with freshly trypsinized Vero cells at 4°C in the presence of sodium azide. A sonic lysate of *E. coli* DH5α served as the negative control. The surface-bound toxins on Vero cells were detected by MAb 4F7, which is specific for the A subunit of Shiga toxin. The detector 1 row shows cells labeled for bound toxins, and the detector 2 row shows the same cells labeled with the membrane lipid probe dil. (A) *E. coli* DH5α lysate. (B) Mutant Shiga R33C. (C) Mutant Shiga A43T. (D) Mutant Shiga G60D. (E) Wild-type Shiga toxin. Each panel shows a single representative field.

widely used to analyze the structure-function relationships of cloned gene products. This technique has been applied most often to the study of proteins for which no three-dimensional structural information is available (27). In the present paper, we describe a simple strategy for generating gapped duplex DNA, in which both sense and antisense strands of the target gene segment are mutagenized simultaneously (Fig. 2). This strategy is applicable to any cloned gene in which the desired target region is flanked by two unique restriction sites which yield a 5′ overhang and a 3′ overhang at the termini.

To interpret the effects of the various mutations on cytotoxicity and receptor binding, we found it necessary to ensure that the stability of each mutant polypeptide was comparable to that of the wild-type toxin. Two experimental approaches were used to test the stability of these mutants: pulse-chase analysis and assessment of immunoreactivity. Densitometric scanning of the X-ray film of the gels that contained the pulsed-chased B polypeptides of Shiga toxin and the three mutant toxins demonstrated that each of the mutant toxins was as stable as was the wild-type Shiga toxin (Fig. 3). We were not able to interpret the pulse-chase results with SLT-II because SLT-II comigrated with other polypeptides (see Results). The fact that SLT-II A42T and SLT-II G59D were immunoreactive although not cytotoxic (Table 2) supports the conclusion that these two mutants were stable, because the quantity of wild-type SLT-II or Shiga toxin required to produce a visible spot in the dot blot ELISA was at least 100-fold greater than the amount required to elicit a cytotoxic response in Vero or HeLa cells (Table 2, footnotes *b* and *c*).

The three SLT-II mutants were completely devoid of any detectable cytotoxicity, but the comparable mutations in Shiga toxin retained detectable, although reduced, cytotoxic activity. It is possible that these mutations affected both toxin molecules similarly but that, because of the wide disparity in the cytotoxicity levels of the wild-type SLT-II and Shiga toxin constructs (Table 2), a mutation which reduces cytotoxicity by 10,000-fold may still elicit a detectable cytotoxic response to Shiga toxin. A similar explanation can be proposed for the negative results obtained with SLT-II mutants in the receptor analog-binding assay, TLC overlay assay, and Vero cell-binding assay (Table 3); the binding of these SLT-II mutants may have been below the threshold level of sensitivity of these assays. Alternatively, identical mutations may affect Shiga toxin and SLT-II differently. In interpreting the mutational effects on cytotoxicity, we found it critical to ensure that the stability of the mutant polypeptides was comparable to that of the wild-type toxin. Densitometric scanning analysis of the pulsed-chased mutant B polypeptides of Shiga toxin revealed no significant loss of stability when compared with the stability of the wild-type toxin (see Fig. 3 legend). The immunoreactivities of the wild-type Shiga toxin and SLT-II were abolished when the concentrated sonic lysates were diluted more than 1,000-fold and tested in the dot blot ELISA (see Table 2, footnotes *b* and *c*), although the cytotoxic titers of these sonic lysates were 10^{10} CD_{50}/ml and 10^5 CD_{50}/ml, respectively. This result illustrates the fact that the quantity of toxin required to elicit detectable immunoreactivity in the dot blot ELISA was far greater than the amount of toxin required to elicit a cytotoxic response in Vero or HeLa cells. Thus, it is conceivable that the lack of any detectable cytotoxic activity in SLT-II mutants which were still immunoreactive may have been due to the attenuation of cytotoxic activity rather than to the instability of the mutant polypeptides.

That MAb 13C4, which recognizes an epitope in the B subunit of Shiga toxin and is capable of neutralizing the cytotoxic activity of Shiga toxin, was still able to recognize receptor analog-bound toxin (Fig. 4) was somewhat surprising. This observation suggests that the epitope reactive with MAb 13C4 remains accessible to the MAb even after the toxin-receptor interaction has taken place and that the toxin-neutralizing capacity of MAb 13C4 is due to a mechanism other than interruption of the toxin-receptor interaction. Alternatively, since the Shiga toxin B subunit is multivalent, some of the monomers may be involved in receptor binding while others remain accessible to MAb 13C4. It should also be noted that when the toxin-receptor interaction occurred, some epitopes of the A subunit of Shiga toxin remained accessible to antibodies, as demonstrated in the immunofluorescence assay (Fig. 6).

When arginine was replaced by cysteine, mutant Shiga R33C toxin reacted with all three MAb. This finding indicates that R33 is not critical for maintaining a conformation with an exposure of immunoreactive epitopes. However, this mutation produced the most profound reduction in cytotoxicity. It is tempting to speculate that R33 in the B subunit of Shiga toxin may be directly involved in forming the binding site for the interaction with Gb_3. The recent findings of Surewicz et al. (32) support the idea that this region of the Shiga toxin B polypeptide is involved in toxin-receptor interactions. These investigators reported that W34 is in close proximity to the receptor-binding domain of the B subunit of Shiga toxin, as determined by fluorescence spectroscopy. The analogous arginine in the SLT-II B polypeptide (R32) may play a similar role. Although we were unable to rule out the possibility that the R32C mutation in SLT-II is unstable by pulse-chase analysis, the mutant did induce cytotoxin-neutralizing antibodies in rabbits.

Mutant Shiga A43T is of special interest, because a relatively conservative substitution led to a significant alteration in the tertiary structure of the toxin molecule, as indicated by immunoreactivity profiles in the dot blot ELISA (Table 2). On the basis of the receptor analog ELISA (Fig. 4) and TLC overlay assay (Fig. 5) results, it appears that the A43T mutation affected the binding of the Shiga toxin B subunit to the Gb_3 receptor. However, it should be noted that the cytotoxicity was affected less by this mutation than by the other two Shiga toxin mutations (Table 2). Subunit assembly and holotoxin formation as well as ability to bind to Vero cells did not appear to be affected by this mutation, as determined by the immunofluorescence assay (Fig. 6). The possibility exists that the A43T mutation induced a conformational change compatible with high-avidity interactions with a nonglycolipid molecule on the cell surface, such as a glycoprotein. Such a change would still result in a strong reaction in the immunofluorescence assay. This possibility is particularly intriguing in light of reports showing avid interactions of Shiga toxin and SLT-II with glycoproteins (1, 14). The inability of mutant Shiga A43T to bind strongly to the functional Gb_3 receptor on the cell surface may be responsible for the reduced cytotoxicity of Mutant Shiga A43T.

The immunoreactivity profile of mutant Shiga G60D indicates that the epitope reactive with MAb 19G8 was disrupted by the G60D mutation in the B subunit of Shiga toxin. This mutation also affected the receptor interaction. That the effect of this mutation on the receptor interaction may be to reduce the avidity of the receptor-ligand interaction is suggested by the dose-response curve generated in the receptor analog ELISA (Fig. 4). In addition to suboptimal binding to the functional receptor, a failure to traverse the cytoplasmic

membrane efficiently is a possibility which could contribute to the reduced cytotoxic activity of this mutant.

ACKNOWLEDGMENTS

We thank P. Y. Perera (Department of Microbiology, U.S.U.H.S.) and T. Sellner (Laser Biophysics Center, U.S.U.H.S.) for advice and assistance with the ACAS 470.

This work was funded by Public Health Service grant AI 20148-06 from the National Institutes of Health and Uniformed Services University of the Health Sciences protocol R73AK-01.

REFERENCES

1. **Acheson, D. W. K., G. T. Keusch, M. Lightowles, and A. Donohue-Rolf.** 1990. Enzyme-linked immunosorbent assay for Shiga toxin and Shiga-like toxin II using P_1 glycoproteins from hydatid cysts. J. Infect. Dis. **161**:134–137.
2. **Bowie, J. U., and R. T. Sauer.** 1989. Identification of C-terminal extensions that protect proteins from intracellular proteolysis. J. Biol. Chem. **264**:7596–7602.

2a. **Boyd, B., and J. Gariepy.** 1990. Abstr. Annu. Meet. Am. Soc. Microbiol. 1990, B-197, p. 59.

3. **Donohue-Rolf, A., M. Jacewicz, and G. T. Keusch.** 1989. Isolation and characterization of functional Shiga toxin subunits and renatured holotoxin. Mol. Microbiol. **3**:1231–1236.
4. **Downes, F. P., T. J. Barrett, J. H. Green, C. H. Aloisio, J. S. Spika, N. A. Strockbine, and I. K. Wachsmuth.** 1988. Affinity purification and characterization of Shiga-like toxin II and production of toxin-specific monoclonal antibodies. Infect. Immun. **56**:1926–1933.
5. **Endo, Y., K. Tsurugi, T. Yutsudo, Y. Takeda, K. Ogasawara, and K. Igarashi.** 1988. Site of action of a Verotoxin (VT2) from *Escherichia coli* O157:H7 and Shiga toxin on eukaryotic ribosomes. Eur. J. Biochem. **171**:45–50.
6. **Gentry, M. K., and J. M. Dalrymple.** 1980. Quantitative microtiter cytotoxicity assay for *Shigella* toxin. J. Clin. Microbiol. **12**:361–366.
7. **Griffin, D. E., M. K. Gentry, and J. E. Brown.** 1983. Isolation and characterization of monoclonal antibodies to Shiga toxin. Infect. Immun. **41**:430–433.
8. **Hanahan, D.** 1985. Techniques for transformation of *E. coli*, *In* p. 109–135. DNA cloning: a practical approach, vol. 1. IRL Press, Oxford.
9. **Harari, I., A. Donohue-Rolfe, G. Keusch, and R. Arnon.** 1988. Synthetic peptides of Shiga toxin B subunit induce antibodies which neutralize its biological activity. Infect. Immun. **56**:1618–1624.
10. **Hogan, M. M., P. Y. Perera, and S. N. Vogel.** 1989. Examination of macrophage cell surface antigen regulation by rIFN α and IFN α/β utilizing digital imaging by a novel laser detection system: anchored cell analysis station (ACAS) 470. J. Immunol. Methods **123**:9–18.
11. **Jacewicz, M., H. Clausen, E. Nudelman, A. Donohue-Rolfe, and G. T. Keusch.** 1986. Pathogenesis of *Shigella* diarrhea. XI. Isolation of a *Shigella* toxin binding glycolipid from rabbit jejunum and HeLa cells and its identification as globotriaosylceramide. J. Exp. Med. **163**:1391–1404.
12. **Jackson, M. P., R. J. Neil, A. D. O'Brien, R. K. Holmes, and J. W. Newland.** 1987. Nucleotide sequence analysis and comparison of the structural genes for Shiga-like toxin I and Shiga-like toxin II encoded by bacteriophages from *Escherichia coli* 933. FEMS Microbiol. Lett. **44**:109–114.
13. **Jackson, M. P., E. A. Wadolkowski, D. L. Weinstein, R. K. Holmes, and A. D. O'Brien.** 1990. Functional analysis of the Shiga toxin and Shiga-like toxin type II variant binding subunits by using site-directed mutagenesis. J. Bacteriol. **172**:653–658.
14. **Keusch, G. T., M. Jacewicz, and A. Donohue-Rolfe.** 1986. Pathogenesis of *Shigella* diarrhea. Evidence for an *N*-linked glycoprotein receptor and receptor modulation by β-galactosidase. J. Infect. Dis. **153**:238–248.
15. **Knowles, J. R.** 1987. Tinkering with enzymes: what are we learning? Science **236**:1252–1258.
16. **Kunkel, T. A., J. D. Roberts, and R. A. Zakour.** 1987. Rapid and efficient site-specific mutagenesis without phenotypic selection. Methods Enzymol. **54**:367–382.
17. **Lindberg, A. A., J. E. Brown, N. Stromberg, M. Westling-Ryd, J. E. Schultz, and K. A. Karlsson.** 1987. Identification of the carbohydrate receptor for Shiga toxin produced by *Shigella dysenteriae* type I. J. Biol. Chem. **262**:1779–1785.
18. **Lingwood, C. A., H. Law, S. Richardson, M. Petric, J. L. Brunton, S. De Grandis, and M. Karmali.** 1987. Glycolipid binding of purified and recombinant *Escherichia coli* produced Verotoxin *in vitro*. J. Biol. Chem. **262**:8834–8839.
19. **Maniatis, T., E. F. Fritsch, and J. Sambrook.** 1989. Molecular cloning: a laboratory manual. Cold Spring Harbor Laboratory, Cold Spring Harbor, N.Y.
20. **Marques, L. R. M., J. S. M. Peiris, S. J. Cryz, and A. D. O'Brien.** 1987. *Escherichia coli* strains isolated from pigs with edema disease produce a variant of Shiga-like toxin II. FEMS Microbiol. Lett. **44**:33–38.
21. **Mobassaleh, M., A. Donohue-Rolf, M. Jacewicz, R. J. Grand, and G. T. Keusch.** 1988. Pathogenesis of *Shigella* diarrhea. XIII. Evidence for a developmentally regulated glycolipid receptor for *Shigella* toxin involved in the fluid secretory response of rabbit small intestine. J. Infect. Dis. **157**:1023–1031.
22. **Newland, J. W., N. A. Strockbine, and R. J. Neill.** 1987. Cloning of genes for production of *Escherichia coli* Shiga-like toxin type II. Infect. Immun. **55**:2675–2680.
23. **Perera, L. P., L. R. M. Marques, and A. D. O'Brien.** 1988. Isolation and characterization of monoclonal antibodies to Shiga-like toxin II of enterohemorrhagic *Escherichia coli* and use of the monoclonal antibodies in a colony enzyme-linked immunosorbent assay. J. Clin. Microbiol. **26**:2127–2131.
24. **Samuel, J. E., L. P. Perera, S. Ward, A. D. O'Brien, V. Ginsburg, and H. C. Krivan.** 1990. Comparison of the glycolipid receptor specificities of Shiga-like toxin type II and Shiga-like toxin type II variants. Infect. Immun. **58**:611–618.
25. **Sancar, A., A. M. Hack, and W. D. Rupp.** 1979. Simple method for identification of plasmid-coded proteins. J. Bacteriol. **137**:692–693.
26. **Sancar, A., R. P. Wharton, S. Seltzer, B. M. Kacinski, N. D. Clarke, and W. D. Rupp.** 1981. Identification of the *uvrA* gene product. J. Mol. Biol. **148**:45–62.
27. **Shortle, D.** 1987. Genetic strategies for analysing proteins, p. 103–108. *In* D. L. Oxander and C. F. Fox (ed.), Protein engineering. Alan R. Liss, Inc., New York.
28. **Shortle, D., and D. Botstein.** 1983. Directed mutagenesis with sodium bisulfite. Methods Enzymol. **100**:457–468.
29. **Strockbine, N. A., M. P. Jackson, L. M. Sung, R. K. Holmes, and A. D. O'Brien.** 1988. Cloning and sequencing of the genes for Shiga toxin from *Shigella dysenteriae* type I. J. Bacteriol. **170**:1116–1122.
30. **Strockbine, N. A., L. R. M. Marques, R. K. Holmes, and A. D. O'Brien.** 1985. Characterization of monoclonal antibodies against Shiga-like toxin from *Escherichia coli*. Infect. Immun. **50**:695–700.
31. **Strockbine, N. A., L. R. M. Marques, J. W. Newland, H. W. Smith, R. K. Holmes, and A. D. O'Brien.** 1986. Two toxin-converting phages from *Escherichia coli* O157:H7 strain 933 encode antigenically distinct toxins with similar biologic activities. Infect. Immun. **53**:135–140.
32. **Surewicz, W. K., K. Surewicz, H. H. Mantsch, and F. Auclair.** 1989. Interaction of Shigella toxin with globotriaosyl ceramide receptor-containing membranes: a fluorescence study. Biochem. Biophys. Res. Commun. **160**:126–132.

32a. **Tyrrell, G., K. Ramotar, C. Lingwood, and J. L. Brunton.** 1990. Abstr. Annu. Meet. Am. Soc. Microbiol. 1990, B-195, p. 59.

33. **Weinstein, D. L., M. P. Jackson, L. P. Perera, R. K. Holmes, and A. D. O'Brien.** 1989. In vivo formation of hybrid toxins comprising Shiga toxin and Shiga-like toxins and role of the B subunit in localization and cytotoxic activity. Infect. Immun. **57**:3743–3750.
34. **Weinstein, D. L., M. P. Jackson, J. E. Samuel, R. K. Holmes, and A. D. O'Brien.** 1988. Cloning and sequencing of a Shiga-like toxin type II variant from an *Escherichia coli* strain responsible for edema disease of swine. J. Bacteriol. **170**:4223–4230.